**A COMPREHENSIVE VIEW OF THE STRATIGRAPHY AND MINERALOGY OF CHLORIDE-BEARING AND HYDRATED UNITS IN NOACHIS TERRA, MARS.** B. P. Phillips[1], T. D. Glotch[1], A. D. Rogers[1], M. M. Osterloo[2], [1]Department of Geosciences, Stony Brook University, Stony Brook, NY (brooke.phillips@stonybrook.edu), [2]Laboratory for Atmospheric and Space Physics, Boulder, CO.

**Introduction:** Numerous chloride–bearing deposits (~600) have been detected on Mars using data from the Mars Odyssey Thermal Emission Imaging System (THEMIS) [1-4], however, few have been studied in detail [1] and only one site [5] has been placed into the regional geologic context and stratigraphy. The chloride deposits appear to be thermophysically distinct and exhibit relatively featureless red spectral slopes in the visible near infrared (VNIR) and blue slopes superimposed on typical basaltic regolith in the mid–infrared (MIR), consistent with a mixture of anhydrous chlorides and silicates [1, 2]. The chlorides' dominant formation mechanism is likely to be precipitation and/or evaporation from ponded surface runoff or groundwater upwelling [1, 4, 5]. In terrestrial settings, chloride deposits are associated with other alteration or evaporite phases, such as phyllosilicates and sulfates [4]. On Mars, however, additional evaporites have yet to be detected in association with the chloride deposits [3] and only a few occurrences of coexisting phyllosilicate and chloride salt deposits have been detected [1, 4, 6]. Investigations into the role of local and/or regional mechanisms that operated to deposit these unique materials will provide valuable insight into the timing and conditions of past aqueous events on Mars. In particular, this study focuses on the Noachis Terra region where the largest number of chloride deposits have been detected [1].

**Data Reduction and Methodology:** In this study, infrared (IR) spectra from CRISM image FRT00009ACE were atmospherically corrected for both gases and aerosols using the Discrete Ordinate Radiative Transfer (DISORT) model, following the methods of [8]. In the DISORT calculations, single-scattering albedo (SSA) values are acquired under the assumption that the lower boundary of the atmosphere is surface scattering light according to the Hapke function [9]. SSA spectra can be converted back into radiance coefficients comparable to laboratory reflectance [8] assuming incidence and emergence angles of 30° and 0°, respectively. In order to understand surface morphology and stratigraphy associated with local mineralogy (~10 km$^2$ area), CRISM data were co-registered with imaging datasets and projected over rendered digital elevation/terrain models from the Context Imager (CTX) and from the HiRISE instrument (**Figure 2b**) onboard the Mars Reconnaissance Orbiter.

*CRISM spectral end–members*: The relatively flat spectral signatures of anhydrous chloride mostly correspond to mixtures of halite (NaCl) and basaltic dust, likely of eolian origin [2, 6]. The lack of spectral features in the VNIR make the salts difficult to detect using common orbital techniques (i.e. CRISM browse parameters [7]). Through the use of a statistical principal–component approach, known as factor analysis and target transformation (FATT), CRISM spectral end–members were derived from the DISORT corrected image cube [8, 13] and fit to laboratory spectra using a linear least–squares model [11]. Best–fit FATT model results are considered to be the likely spectral end-members in the scene. **Figure 1a** shows best-fit models for hydrated mineral phases. Additionally, CRISM map projected targeted reduced data (MTRDR) data were acquired and ratioed spectra were collected for the various units of interest. MTRDR data aligns both long (IR) and short (VNIR) FRT spectral channels into a single map-projected image, allowing for spectral analysis of prominent spectral signatures at shorter wavelengths. See **Figure 1b** for example.

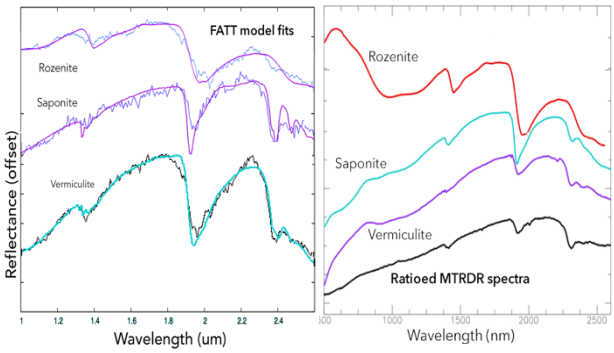


**Figure 1.** CRISM spectral analysis of potential hydrated phases: **(a)** Best-fit FATT model results; **(b)** Comparison of ratioed MTRDR spectra to initial FATT model fits; rozenite does not show a good fit.

*Spectral unmixing of CRISM SSA:* Mineral end-members that have relatively broad and/or featureless single scattering albedo (SSA) are difficult to accurately model (i.e. halite). Consequently, we focus on spectral unmixing of diagnostic primary and secondary mineral phases that are located within the chloride study area to better constrain the composition of and the possible formation mechanisms from which the chloride deposits formed. Additionally, grain size is not a free parameter for the model, therefore, grain combinations are chosen for each unmixing model using derived mineral grainsizes and knowledge of physical geology. In order

to improve signal to noise ratios, regions of ~10 × 10 pixel were averaged.

**Results:** We conducted a detailed compositional and stratigraphic analysis of chloride-bearing deposits in Noachis Terra (**Figure 2a-c**). Three major compositional units have been identified. Initial results show an Fe/Mg-phyllosilicate component, most likely vermiculite, as the dominant alteration phase surrounding the chloride deposits. Derived quantitative abundances of the hydrated phyllosilicate unit range from ~7.0 to 28.5% by volume along the profile line (shown in **Figure 2a)**, RMS values for the spectral fits are less than 0.0040. A pyroxene-rich mafic deposit is suggested for the upper unit, with mineral abundances ranging from ~44.2 to ~61.0% for low-Ca pyroxene and ~22.5 to 33.3% for Mg-rich olivine. Minor abundances of plagioclase are also present (~0-1%). The chloride deposits are identified within local topographic lows, embaying the Fe/Mg–phyllosilicate unit, and appearing to be discontinuous, thin layers of relatively consolidated material (**Figure 2c**). Chloride abundances cannot be derived from the unmixing model due to the lack of spectral signatures, but previous modeling and laboratory work has suggested that salt abundances range from ~10-20% [12]. Future work will attempt to further constrain chloride abundances using a combination of manual spectral inspection of CRISM, TES, and THEMIS data with improved laboratory spectra of various mineral mixtures, and geochemical modeling.

The juxtaposition of the observed alteration units suggests the salts occurred subsequent to the formation of the hydrated clays. The local depressions suggest ponding and evaporation of surface water runoff and/or ground water discharge, consistent with previously inferred formation mechanisms [1, 5]. A tributary channel terminates at the topographic low where the chloride deposits have been detected. Fluvial channels crosscut the subdivided highland units and provide supplementary constraints on the timing and potential source of surface runoff. A local topographic profile of the units (**Figure 2b**) was extracted from HiRISE DTM, *DTEEC_007058_1745_016354_1745_U01,* allowing for interpretation of the stratigraphic relations between the identified units.

**Discussion and Future Work:** Spectral unmixing of retrieved SSA can be used to derive mineral abundances at fine resolutions, however, selection of an end-member library is the dominant constraint on the utility of the unmixing model. Updating the spectral library is a continuous process and is necessary for improving model results. Continued efforts to map the Noachis Terra chloride deposits and associated mineralogy at local and regional scales will provide an enhanced understanding of the geochemical and the geophysical processes that have shaped the southern highlands on Mars.

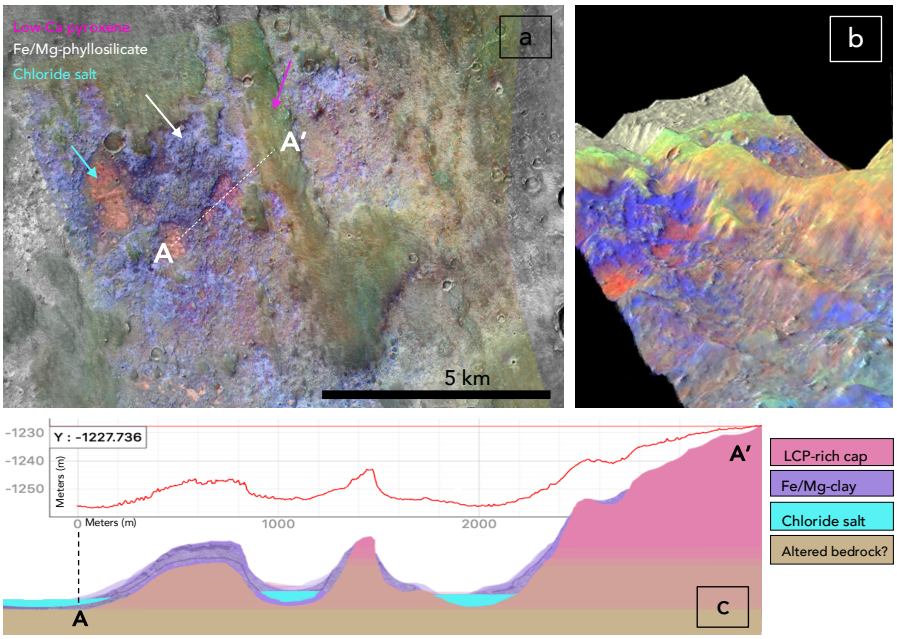


**Figure 2. (a)** FRT0009ACE over HiRISE imagery; RGB displayed using summary products [7]: inverse ISLOPE, LCPINDEX, and BDI1000IR; **(b)** HiRISE DTM with 15x exaggeration, shows stratigraphic relationships of identified units; **(c)** Topographic profile (A-A') marked by dashed white line in (a) and identified stratigraphic of units.

**References:** [1] Osterloo, M. M. et al. (2010) *JGR*, 115, E10. [2] Jensen, H. B. and Glotch, T. D. (2011) *JGR*, 116, E12. [3] Murchie, S. L. et al. (2009) *JGR*, 114, E2. [4] Glotch, T. D. (2010) *GRL*, 37, 16. [5] Hynek, B. M. et al. (2015) *Geology*, 43, 787-790. [6] Ruesch, O. et al. (2012) *JGR*, 117, E00J13. [7] Viviano–Beck, C. E. et al. (2014) *JGR,* 119, 1403-1431. [8] Liu, Y. et al. (2016) *JGR*, 121, 2004-2036. [9] Hapke, B. (2012) *Cambridge Univ. Press.* [10] Ramsey M. S. and Christensen P. R. (1998) *JGR*, 103, 577-596. [11] Amador, E.S. and Bandfield, J.L.(2016) *Icarus*, 276. [12] Glotch, T. D. et al. (2016) *JGR*, 121, 454-471. [13] Thomas, N. H. and Bandfield, J. L. (2013) *LPS XLIV*, Abstract #1325.

**Additional Information:** This work is supported by the NASA Mars Data Analysis Program, #80NSSC17K0671.